Journal of Hazardous Materials 203–204 (2012) 274–282

Contents lists available at SciVerse ScienceDirect

Journal of Hazardous Materials

journal homepage: www.elsevier.com/locate/jhazmat

Preparation and characterization of nano-structured lead oxide from spent lead acid battery paste

Lei Li[a], Xinfeng Zhu[a,b], Danni Yang[a], Linxia Gao[a], Jianwen Liu[a], R. Vasant Kumar[c], Jiakuan Yang[a,*]

[a] School of Environmental Science and Engineering, Huazhong University of Science and Technology (HUST), 1037 Luoyu Road, Wuhan, Hubei, 430074, PR China
[b] Henan University of Urban Construction, Pingdingshan, Henan, 467000, PR China
[c] Department of Materials Science and Metallurgy, University of Cambridge, Cambridge, CB2 3QZ, UK

ARTICLE INFO

Article history:
Received 9 September 2011
Received in revised form 6 December 2011
Accepted 6 December 2011
Available online 14 December 2011

Keywords:
Spent lead acid battery
Nano-structured lead oxide
Lead citrate
Thermal decomposition
Electrochemistry test

ABSTRACT

As part of contribution for developing a green recycling process of spent lead acid battery, a nanostructural lead oxide was prepared under the present investigation in low temperature calcination of lead citrate powder. The lead citrate, the precursor for preparation of this lead oxide, was synthesized through leaching of spent lead acid battery paste in citric acid solution. Both lead citrate and oxide products were characterized by means of thermogravimetric-differential thermal analysis (TG-DTA), X-ray diffraction (XRD), and scanning electron microscope (SEM). The results showed that the lead citrate was sheet-shape crystal of $Pb(C_6H_6O_7)\cdot H_2O$. When the citrate was calcined in N_2 gas, β-PbO in the orthorhombic phase was the main product containing small amount of Pb and C and it formed as spherical particles of 50–60 nm in diameter. On combusting the citrate in air at 370 °C (for 20 min), a mixture of orthorhombic β-PbO, tetragonal α-PbO and Pb with the particle size of 100–200 nm was obtained, with β-PbO as the major product. The property of the nanostructural lead oxide was investigated by electrochemical technique, such as cyclic voltammetry (CV). The CV measurements presented the electrochemical redox potentials, with reversibility and cycle stability over 15 cycles.

1. Introduction

In the past few years, the synthesis of nano-structured oxide materials has attracted considerable attention [1,2] of chemists and metallurgists. Lead oxide has many crystalline forms, such as PbO (α, β), Pb_2O_3, Pb_3O_4, and PbO_2 (α, β). Lead dioxide (PbO_2), which is used as a positive active material in lead acid battery, has been extensively studied. Several electrochemical methods, such as cyclic voltammetry (CV) [3], constant current and constant voltage approaches, have been developed recently to prepare nano-structured PbO_2. Ghasemi et al. [4] used a pulse method for anodic deposition of PbO_2 from solutions containing Pb^{2+} on a substrate. The lead dioxide films prepared were used as positive electrodes in lead acid batteries and maximum capacity was observed when pulse and relaxation time was equal to 0.1 and 5 s. Morales et al. [5] obtained lead dioxide particles ranging from nano-metric to micrometric size by using spray deposition technique.

In lead acid batteries, PbO is the starting precursor paste material for both anode and cathode, which is then converted to active Pb and PbO_2, respectively, during cell formation stage. There is big interest to improve lead oxide characteristics to obtain more discharge capacity and more cycle-life. It is expected that the lead oxide in form of nano-particulates can deliver more electrical energy at discharge process due to its large specific surface area and good reversible property. However, there are only a few reports about the synthesis of nano-size lead oxide. Wang et al. [6] prepared nano crystalline lead oxide through two-step chemical reactions. In his research, the lead oxide was tested as the electrode active material for the valve-regulated lead acid (VRLA) battery. The research results from Cruz et al. [7] showed that α-PbO thin films were prepared by spray pyrolysis of aqueous solutions of $Pb(CH_3COO)_2\cdot 3H_2O$ and deposited onto a lead substrate. The battery cell maintained a discharge capacity of 100 mAh g^{-1} of positive plate (40 wt% of the theoretical value) upon extensive cycling. Karami et al. [8,9] synthesized a uniform nano-structured lead oxide via sonochemical method. The electrochemical tests showed that a large discharge capacity and excellent cycle characteristics of the nanostructured powder were obtained. Salavati-Niasari et al. [10] reported that synthesis of nano-size lead oxide powder with an average particle size of 35 nm could be made by decomposing lead oxalate at 500 °C. Sadeghzadeh et al. [11] used 2-pyridinecarboxylic acid, lead acetate and sodium nitrite to synthesize one-dimensional structure of Pb (II) chelate, which was roasted at 110–500 °C, to produce PbO nanostructures successfully. The influence of atmosphere

* Corresponding author. Tel.: +86 27 87792207; fax: +86 27 87792101.
E-mail addresses: jkyang@mail.hust.edu.cn, yjiakuan@hotmail.com (J. Yang).

0304-3894/$ – see front matter.
doi:10.1016/j.jhazmat.2011.12.021

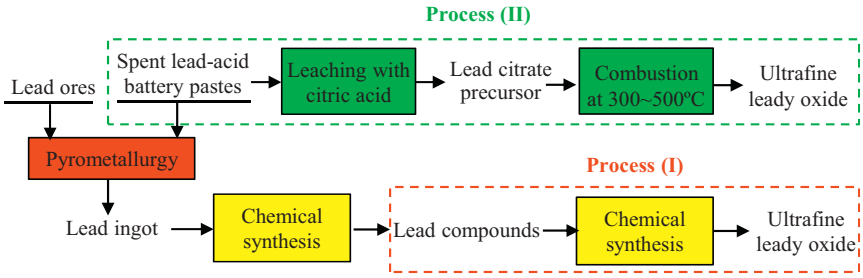

Fig. 1. Different procedures of preparing nanostructured lead oxide. Process (I): the typical preparation process from the starting materials of lead compounds; Process (II): the novel preparation process from the starting materials of spent lead battery paste.

Table 1
Chemical composition of spent lead acid battery paste.

Constituent	$PbSO_4$	PbO_2	PbO	Pb	Others
Percentage (%)	64.5	29.5	4.5	1	0.5

during calcination on the morphology and the exact composition of nanostructured PbO have not been reported.

It is noted from review of the literatures that the previous preparation methods of nanostructured powders, as shown in Fig. 1, can be characterized as the following process route (I): The starting materials are typically lead compounds, such as $Pb(NO_3)_2$, $Pb(CH_3COO)_2{\cdot}3H_2O$. The starting lead compounds are generally produced from either spent lead acid battery pastes or lead ores, both of which are subject to pyrometallurgical process. These processes based on pyrometallurgical process are high-energy consuming, complicated and costly. As pyrometallurgical process of recycling spent lead acid batteries is associated with emission of pollutants such as SO_2 and lead particulates into air/soil environment [12], more and more attentions have been paid to more efficient and environment-friendly alternative processes based on chemical and electrochemical methods [13–17].

As shown in process (II) [15–17], the nanostructured lead oxide was prepared via a low temperature calcination process, by using lead citrate as a precursor which was synthesized from the starting materials of spent lead acid battery paste in citric acid system. In previous literatures [6–11], no results were reported about the preparation of nanostructured lead oxide directly from the spent lead acid battery paste. In this study, nanostructured lead oxide was combustion/calcination-synthesized from lead citrate precursor in both N_2 gas and air, using spent lead acid battery pastes as the starting materials.

2. Experimental

2.1. Chemicals

The samples of spent lead acid battery pastes were provided by Hubei Jinyang Metallurgical Co. Ltd., China, where the waste lead pastes are treated to recover lead metal using a conventional smelting process. The chemical composition of the spent lead acid battery pastes is shown in Table 1.

Citric acid monohydrate ($C_6H_8O_7{\cdot}H_2O$, 99.5% purity) was used to prepare the citric acid aqueous solution with distilled water. Trisodium citrate hydrate ($Na_3C_6H_5O_7{\cdot}2H_2O$, >99% purity) was used as the desulfating agent during leaching of spent lead battery pastes. Hydrogen peroxide (H_2O_2, 30% w/v) was used as the reductant.

2.2. Synthesis of lead citrate

Leaching experiments were carried out under the optimized leaching conditions as described in another paper [18]. 10 g of spent lead battery paste was added to citric acid and trisodium citrate and 30% peroxide hydrogen solution with a solid/liquid mass ratio of 1/5. The mole ratio of reactants was taken as: spent lead acid battery pastes:$C_6H_8O_7{\cdot}H_2O$:$Na_3C_6H_5O_7{\cdot}2H_2O$:$H_2O_2$ = 1.0:1.3:0.9:7.4 and the pH of the solution were in a range of 3–4. Leaching was carried out under magnetic stirring at speed of 650 rpm to maintain full suspension of the slurry for 24 h at room temperature (22 °C). During leaching, lead citrate began to crystallize from the solution at the room temperature. The resulting crystals were washed with distilled water; vacuum filtrated and dried at 65 °C. The concentration of lead ion in the left solution was analyzed with atomic absorption spectrometry (AAS). The recovery of lead and the mass balance of processes were calculated.

2.3. Thermal analyses of lead citrate

Thermal analyses of the lead citrate were performed in corundum crucible by thermogravimetric-differential thermal analysis (TG-DTA), in different atmospheres using TA Instruments (Diamond TG-DTA, Platinum-Selmer equipment Co. Ltd., Shanghai), with air or nitrogen gas under a flow rate of 100 $cm^3\,min^{-1}$ by heating up to 800 °C at heating rate of 5 °C min^{-1}.

2.4. Calcination of lead citrate

In nitrogen gas, the lead citrate powders were calcined at 225 °C, 270 °C, 313 °C and 380 °C for 1 h, respectively, at heating rate of 5 °C min^{-1}. In the air, the citrate powders were calcined at 165 °C, 275 °C, 335 °C, 370 °C, 410 °C, 430 °C and 450 °C for 1 h respectively. The lead citrate powders were also calcined isothermally at 370 °C with variation of time, such as 5 min, 10 min, 20 min, 30 min and 60 min in air. The weight loss was measured for each set of the experiments. Calcination temperature was determined based on TG-DTA data. The ratio of PbO in lead oxide sample was measured by chemical analysis [19].

2.5. Characterization of materials

X-ray diffraction (XRD) data were collected from powder samples using a X'Pert PRO XRD (Philips, PANalytical B.V., Holland) with Cu Kα radiation and λ = 1.5418 Å at scanning rate of 0.28° per second for 2θ in the range from 5° to 75°. Morphology studies were carried out with scanning electron microscopy (Sirion 200SEM, FEI, Holland) operated at 10 kV after coating the samples with gold. EDX spectra of the calcined products were collected on an ultra-thin window (UTW) X-ray detector equipped with Sirion 200 SEM.

2.6. Characterization of lead oxide with electrochemical measurements

Cyclic voltammetry was employed to investigate the electrochemical behavior of the lead oxide. The CV curves were determined with a typical three-electrode system. The working electrode (WE) was prepared from platinum microelectrode which was filled with lead oxide. PbO in contact with concentrated sulfuric acid was converted into $PbSO_4$ which then acted as the electrochemically active precursor in the electrode for formation of PbO_2 via oxidation. A double platinum electrode was used as the counter electrode while $Hg/Hg_2SO_4/K_2SO_4$ (sat.) was, employed as the reference electrode. Sulfuric acid solution at concentration of 3 mol L^{-1} was used as electrolyte. CV was performed for 15 cycles at room temperature (22 °C) using VMP-2 device from USA with a scanning speed of 20 mV s^{-1} in a potential range of −1.2 V to +2 V.

3. Results and discussion

3.1. Crystallization of lead citrate

In this citric acid leaching system, $C_6H_8O_7{\cdot}H_2O$ was used to supply the citric acid aqueous solution with distilled water for the balance of pH and for leaching–crystallization. The reactions are described in Eqs. (1)–(4). In Eq. (2), H_2O_2 acts as a reductant, and Pb(IV) turns into Pb(II) in the acidic condition. In Eq. (3), $Na_3C_6H_5O_7{\cdot}2H_2O$ acts as a desulfating agent, and citric acid solution provides an acid leaching condition which benefits for the desulfuration reaction of lead sulfate in citric acid-sodium citrate buffering solution.

$$PbO + C_6H_8O_7 \cdot H_2O \rightarrow Pb(C_6H_6O_7) \cdot H_2O + H_2O \quad (1)$$

$$PbO_2 + C_6H_8O_7 \cdot H_2O + H_2O_2 \rightarrow Pb(C_6H_6O_7) \cdot H_2O + O_2 + 2H_2O \quad (2)$$

$$3PbSO_4 + 2Na_3C_6H_5O_7 \cdot 2H_2O \xrightarrow{C_6H_8O_7{\cdot}H_2O} Pb_3(C_6H_5O_7)_2 \cdot 3H_2O + 3Na_2SO_4 + H_2O \quad (3)$$

$$Pb_3(C_6H_5O_7)_2 \cdot 3H_2O + C_6H_8O_7 \cdot H_2O \rightarrow 3Pb(C_6H_6O_7) \cdot H_2O + H_2O \quad (4)$$

Mass balance relating to lead acid battery paste in the leaching–crystallization sequence is given in Table 2. The spent solution was diluted in the 1000 ml volumetric flask. Recovery of lead was calculated by subtracting the mass of lead in the spent solution. As shown in Table 2, the recovery of lead is calculated to be 96.0 wt%.

The XRD patterns of the resulting crystals are shown in Fig. 2. None of the original lead phases are observed in the XRD patterns (a), indicating that the reaction undergone completely. Therefore, the desulfurization rate in the leaching process was around 100%. The pattern of XRD almost matches with lead citrate structural data as referenced in the Cambridge Structural Database (CSD) for $Pb(C_6H_6O_7){\cdot}H_2O$. It is preliminarily indicated that the leaching product is a kind of lead citrate, which can be described as $[Pb(C_6H_6O_7)_m]{\cdot}nH_2O$, where the values of m and n have to be deduced experimentally. In Table 2, under assumption that the lead citrate crystal is formed as $Pb(C_6H_6O_7){\cdot}H_2O$, the stoichiometric mass of solid product is almost equal to the actual mass of solid product, and the error is approximately 0.4%, which confirms the resulting crystals is $Pb(C_6H_6O_7){\cdot}H_2O$.

The photograph of the lead citrate product is shown in Fig. 3(a). Lead citrate precursor is white, which is different from the brown

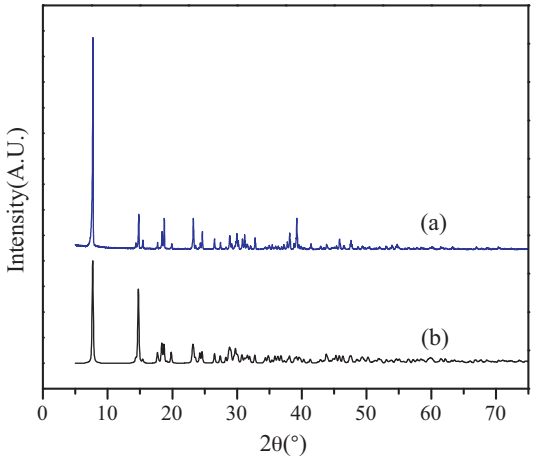

Fig. 2. XRD patterns of (a) crystals obtained from spent lead acid battery pastes, and (b) lead citrate $Pb(C_6H_6O_7){\cdot}H_2O$ from CSD.

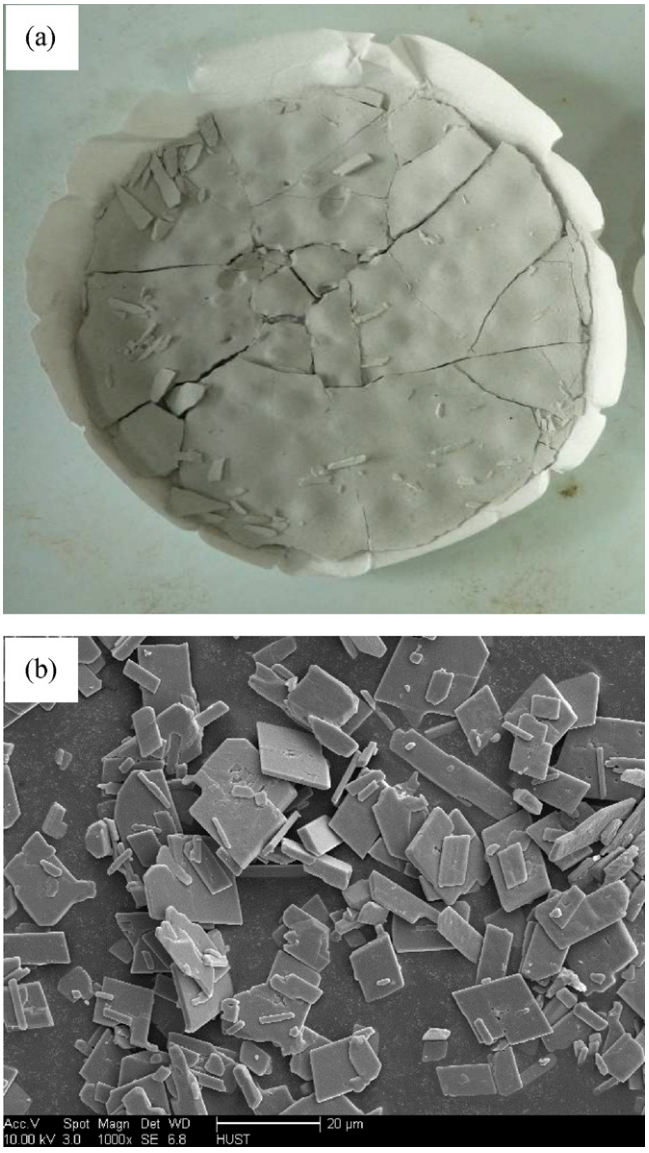

Fig. 3. Photograph and SEM image of lead citrate product: (a) photograph of lead citrate after filtering, and (b) SEM image.

Table 2
Mass of solid products and recovery of lead.

Raw material	Mass of original lead compound (g)	Mass of lead in raw material (g)	Theoretical mass of solid product (g)	Actual of solid product (g)	Mass of lead in the left solution (g)	Recovery of lead (%)
Spent lead acid battery pastes	9.9465	7.4391	14.9141	14.2610	0.2971	96.0

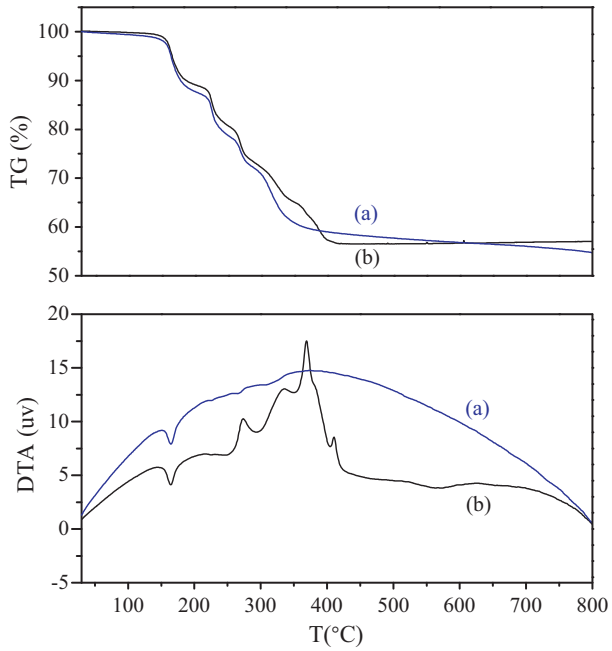

Fig. 4. TG-DTA curves of lead citrate in different atmospheres: (a) in nitrogen gas, and (b) in air.

color of spent lead acid battery paste samples. Morphology of the lead citrate is shown in Fig. 3(b). The lead citrate is sheet shaped with length of 10–20 μm, width of 2–10 μm and thickness of 0.5 μm. These crystals are easy to filter out of the leaching solution.

3.2. Thermal analysis results

Thermal decomposition of lead citrate was identified with thermal analysis. The TG-DTA curves of the lead citrate in two different atmospheres are shown in Fig. 4. Oxygen in air is expected to aid combustion of the citrate precursor, while in the pure nitrogen (oxygen 100 ppm) atmosphere, decomposition of the citrate is supposed to takes place through pyrolysis. From patterns (a), there are four stages of weight loss in the TG curve in N_2, which corresponds to three main endothermic peaks in the DTA curve. The mass loss at 190 °C is approximately 10% which is more than stoichiometric mass loss in dehydration (4.4%). It indicates that both dehydration and decomposition of lead citrate are occurred around 165 °C. Then lead citrate decomposes at 270 °C and 313 °C, respectively. It has been reported that [20] PbO could be reduced to Pb metal by carbon above 370 °C in N_2 gas. As shown in Fig. 4(a), the mass loss keeps increasing slowly when temperature rises from 370 °C to 800 °C. This may be reasoned from the reduction of PbO by carbon. It shows that thermal decomposition of $Pb(C_6H_6O_7)\cdot H_2O$ in N_2 can be completed around and above 380 °C with a total weight loss about 38 wt%. Therefore, the temperature for decomposing lead citrate in nitrogen can be selected progressively near the four stages of weight loss, i.e. 225 °C, 270 °C, 313 °C and 380 °C.

Thermal analysis patterns (b) show that the thermal behavior is more complex in air. In the first stage, weight loss of the lead citrate is observed in the range of 150–180 °C, which is most likely due to dehydration and decomposition, testified by an endothermic peak in the DTA curve. In the following stages, weight loss takes place in the temperature range 270–420 °C, which is ascribed to combustion of the citrate. This process is accompanied by four somewhat overlapping exothermic peaks in DTA curve around 275 °C, 335 °C, 368 °C and 411 °C. Exothermic peaks observed in the DTA curve are ascribed to the oxidation of both C and H from the citrate. When temperature is above 420 °C, both weight loss and heat flow remain constant up to 800 °C. The calcination–combustion temperatures for the citrate can be selected progressively corresponding to the exothermic peaks, at 165 °C, 275 °C, 335 °C, 370 °C, 410 °C, 430 °C and 450 °C.

According to Fig. 4, when temperature is under 370 °C, the TG curve in air is similar to TG in N_2, and the peak temperatures of DTA curve in air is identical to the results in N_2. When temperature is in range of 370–450 °C, the TG curve in air shows a slope, while TG curve in N_2 is an approximately flat line. It can be inferred that there are two stages taking place in the calcination of $Pb(C_6H_6O_7)\cdot H_2O$ in air. One stage is decomposition of citrate which is alike of pyrolysis of citrate in N_2, accompanying by oxidation of a little of C and H; second stage is violent combustion of C and H when the temperature is higher than 370 °C.

3.3. Calcination in nitrogen gas

The samples of lead citrate were heat treated respectively in a tube furnace under nitrogen atmosphere at 225 °C, 270 °C, 313 °C and 380 °C for 1 h to investigate the thermal decomposition. Pictures of calcination products are shown in Fig. 5. Some gas bubbles can be observed, which result from gas generation in the thermal decomposition.

Effect of the calcination temperature on weight loss of the citrate precursor is shown in Fig. 6. The weight loss increases with an increase in calcination temperature from 225 °C to 313 °C and it appears to be a plateau above 380 °C. The weight loss at 380 °C was 37.5 wt%.

The phase transformation of the calcination products was examined with X-ray diffraction technique and is shown in Fig. 7. The product was amorphous at 225 °C, and transformed into crystalline phases at higher temperature. The XRD demonstrates that the crystalline contains massicot (β-PbO) and lead metal at 270 °C. The relative intensity of the peak of β-PbO increases as the calcination temperature is increased. When temperature is higher than 313 °C, β-PbO is the only crystalline phase in the calcination product.

The scanning electron microscope (SEM) images and EDX spectra are shown in Figs. 8 and 9. The products decomposed at 313 °C show two morphologies – spherical particles in the 50–60 nm range with underlying sheets similar to the citrate sheets. Some carbon was identified in calcination product by the EDX spectra. Therefore, the observed mass loss in nitrogen gas is about 7–10% less than the stoichiometric mass loss of 46.2% in the decomposition $Pb(C_6H_6O_7)\cdot H_2O$ to PbO because of the formation of carbon in the decomposition products.

Brown [21] studied the thermal decomposition of lead citrate $Pb_3(C_6H_5O_7)_2\cdot 2H_2O$ in N_2, and the results at temperature (305–325 °C) in his report showed that the pyrophoric metallic lead and carbon particles were produced. However, in this study, a mixture of PbO, Pb and C was obtained as the product of the thermal decomposition of $Pb(C_6H_6O_7)\cdot H_2O$ in inert atmosphere. The presence of carbon is detrimental for making new pastes. Thus

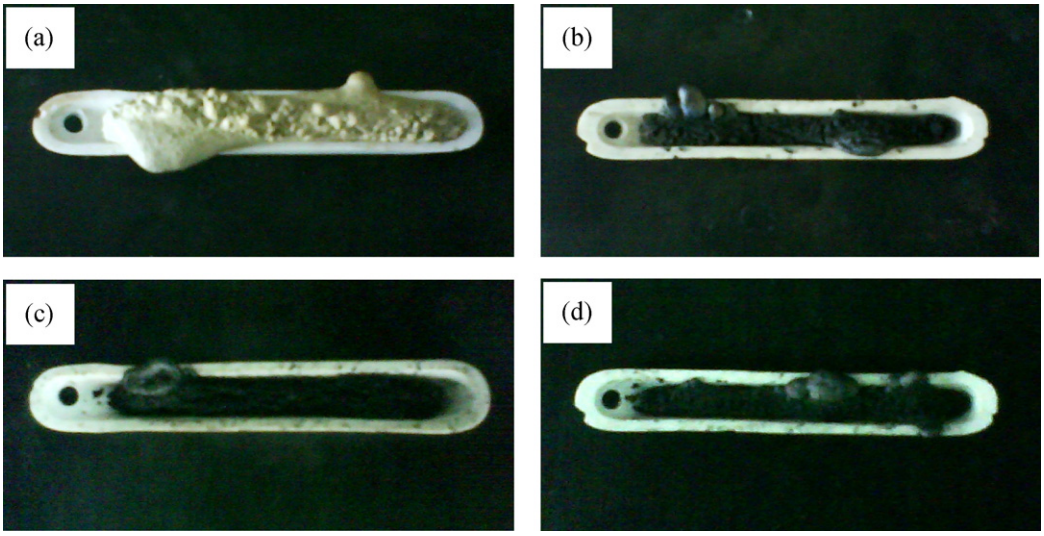

Fig. 5. Photographs of decomposition products from lead citrate after heating in N_2 for 1 h at different temperature: (a) 225 °C, (b) 270 °C, (c) 313 °C, and (d) 380 °C.

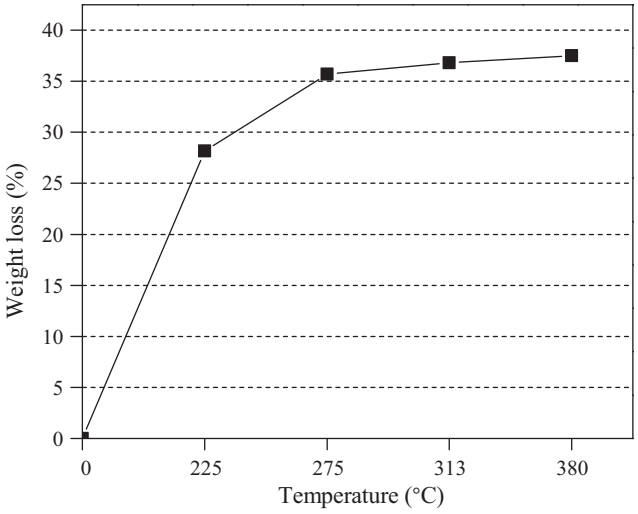

Fig. 6. Effect of calcination temperatures on weight loss of lead citrate in N_2.

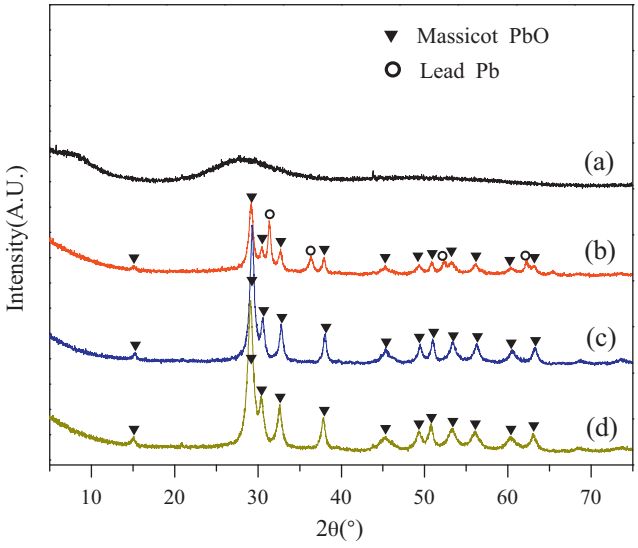

Fig. 7. XRD patterns of decomposition products from lead citrate at different temperature for 1 h in N_2: (a) 225 °C, (b) 270 °C, (c) 313 °C, and (d) 380 °C.

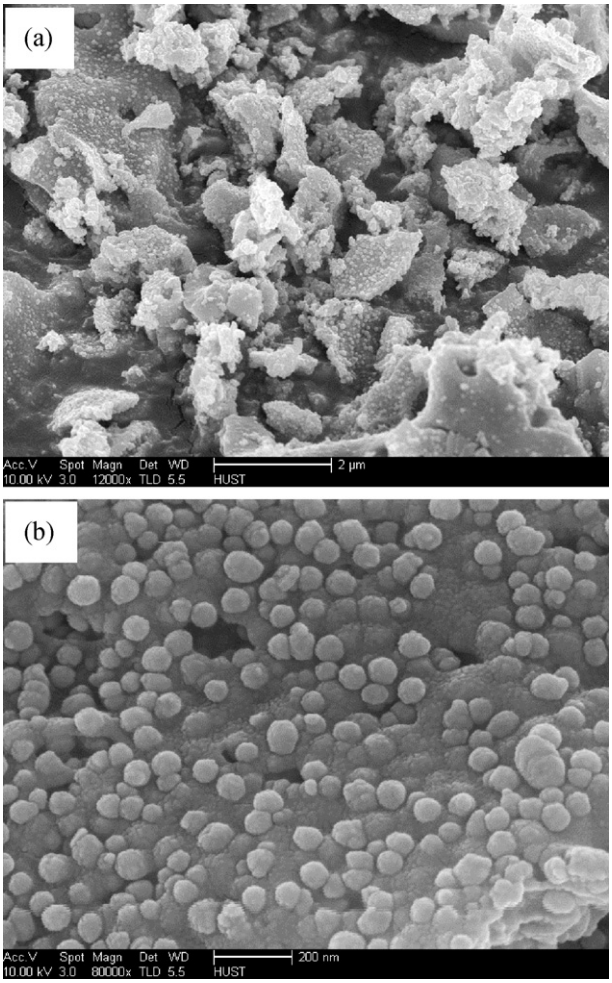

Fig. 8. SEM images of calcination product at 313 °C for 1 h in N_2 at different magnification: (a) 12,000× and (b) 80,000×.

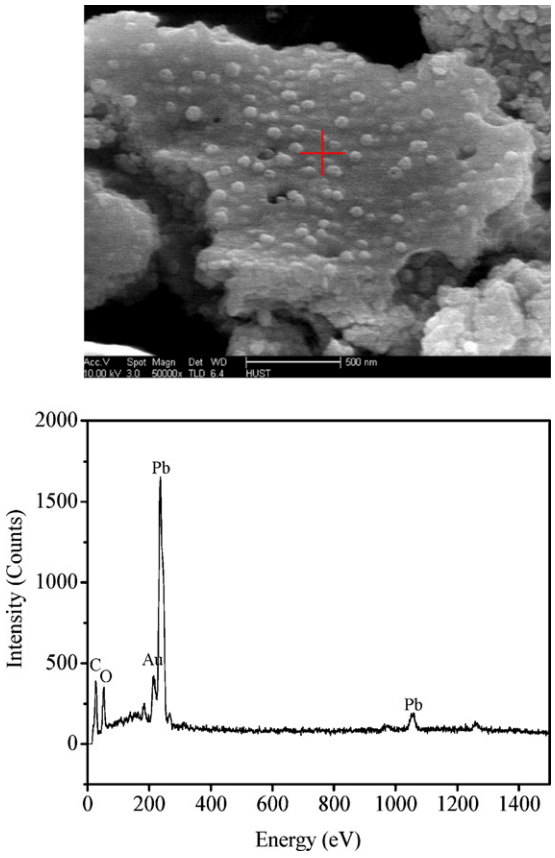

Fig. 9. EDX spectroscopy of calcination product at 313 °C for 1 h in N_2.

decomposition of lead citrate in inert atmosphere is not considered a viable option.

3.4. Calcination in air

In air, lead citrate was calcined respectively for 1 h at 165 °C, 275 °C, 335 °C, 370 °C, 410 °C, 430 °C and 450 °C to remove all carbon and hydrogen. Fig. 10 shows how the appearance of combustion

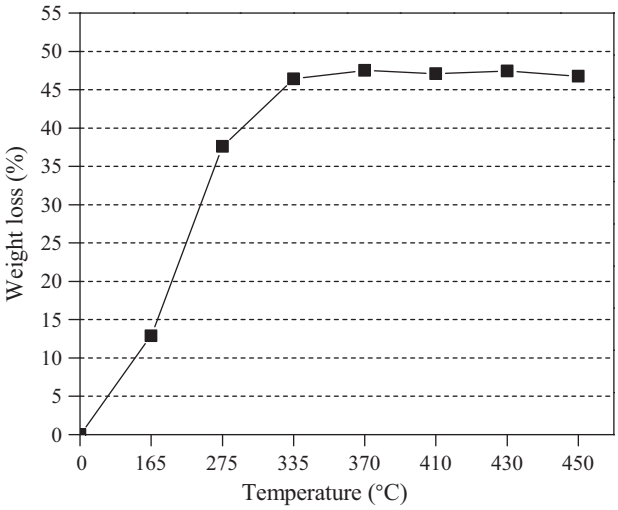

Fig. 11. Effect of calcination temperatures on weight loss after calcinations in air (1 h).

products changes with temperature. The product at 275 °C has a blackish tinge, indicating that the organics of lead nitrate was partially carbonized during the pyrolysis. The color of product turns yellow at and above 335 °C.

The effect of temperature on weight loss of the citrate precursor was investigated. Fig. 11 shows that the weight loss increases with an increase in temperature from 165 °C to 370 °C and then it keeps relatively stable at 47 wt% in the temperature range 370–450 °C.

If air supply is sufficient, PbO is the final product. The decomposition could be shown as Eq. (5). The stoichiometric weight loss in Eq. (5) is 46.2%.

$$Pb(C_6H_6O_7)\cdot H_2O + 4.5O_2 \rightarrow PbO + 6CO_2 + 4H_2O \quad (5)$$

If the air is insufficient, Pb is the final product. The decomposition could be shown as Eq. (6). The stoichiometric weight loss in Eq. (6) is 50.0%.

$$Pb(C_6H_6O_7)\cdot H_2O + 4O_2 \rightarrow Pb + 6CO_2 + 4H_2O \quad (6)$$

The weight loss in the calcination experiments in air is around 47%, which is between 46.2% and 50.0%. It is indicated that the

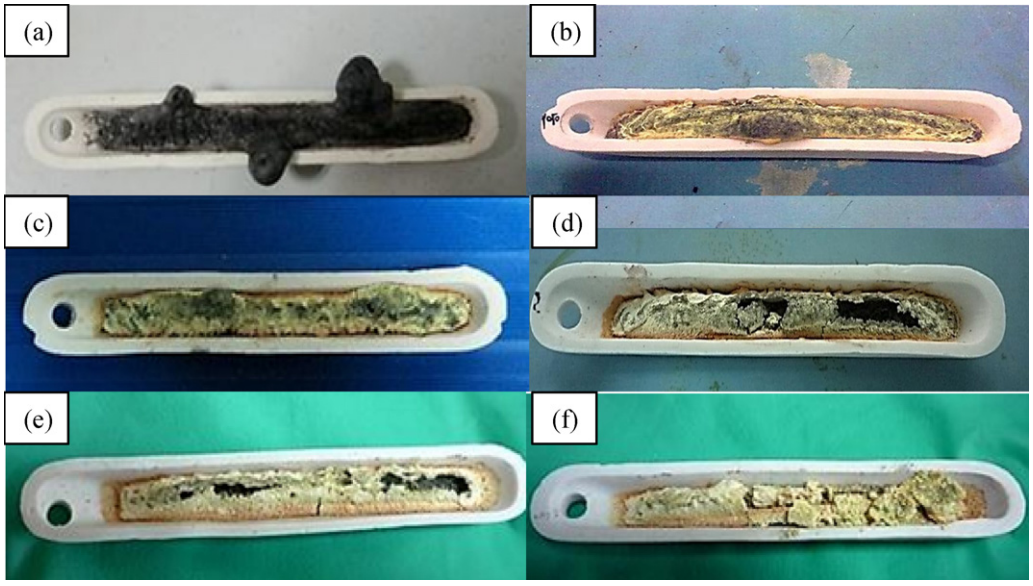

Fig. 10. Photographs of calcination–combustion products at different temperature for 1 h in air: (a) 275 °C, (b) 335 °C, (c) 370 °C, (d) 410 °C, (e) 430 °C, and (f) 450 °C.

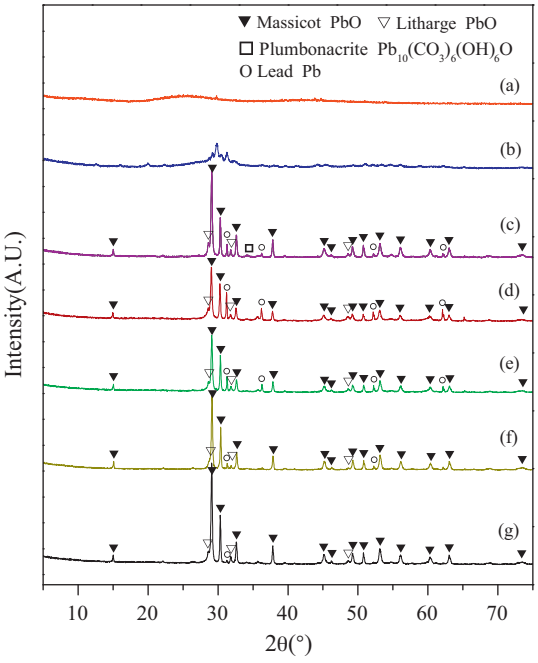

Fig. 12. XRD patterns of calcination–combustion products at different temperature for 1 h in air: (a) 165 °C, (b) 275 °C, (c) 330 °C, (d) 370 °C, (e) 410 °C, (f) 430 °C, and (g) 450 °C.

product was composed of PbO and Pb. The XRD patterns of products (Fig. 12) also demonstrate the composition of PbO and Pb.

Fig. 12 presents the XRD patterns of the calcination products in air at different temperature. The product was amorphous at 165 °C. Obviously, higher temperature transformed the product into crystalline phase of β-PbO. The combustion products were β-PbO, α-PbO and metallic lead at 335 °C, 370 °C, 410 °C, 430 °C and 450 °C, with some intermediate phases at 335 °C. This results suggest that $Pb(C_6H_6O_7)\cdot H_2O$ can be fully calcined in air at and above 370 °C.

Based on the results calcined both in N_2 and in air as mentioned above, it can be confirmed that there are two sequential stages taking place in the calcination of $Pb(C_6H_6O_7)\cdot H_2O$ in air. When temperature is under 370 °C, lead citrate is decomposed and transformed into crystalline phases of β-PbO, α-PbO, Pb and small amount of organic intermediate. The decomposition of this stage is alike of pyrolysis of lead citrate in N_2. Compared to calcination products in N_2 (shown in Fig. 7), the difference is that metallic Pb is mostly oxidized to α-PbO in air. As temperature is higher than 370 °C, C and H in the organic intermediate is combusted violently, accompanied with intense exothermic phenomenon. The temperature of 370 °C leads to producing β-PbO, α-PbO and a little of metallic Pb, and weight loss is 47.5 wt%. The calcination results in N_2 show that the amount of β-PbO increases as the temperature is increased, so does it in air. If temperature is higher than 488 °C, α-PbO will be transformed into β-PbO [22].

Salavati-Niasari et al. [10] prepared PbO nanocrystals via decomposition of lead oxalate in air. He reported that a mixture of α-PbO and β-PbO nanocrystals was obtained at 235 °C, and the proportion of β-PbO increased as the temperature increased. Jia [23] synthesized single crystalline β-PbO nanorods through a hydrothermal processing of $Na_3C_6H_5O_7\cdot 2H_2O$ and $Pb(CH_3COO)_2\cdot 3H_2O$. With lead citrate, formation of β-PbO rather than α-PbO was observed, in both air (by combustion) and N_2 (by decomposition).

The SEM images of the products from the citrate calcined at different temperature in the current research are shown in Fig. 13. The

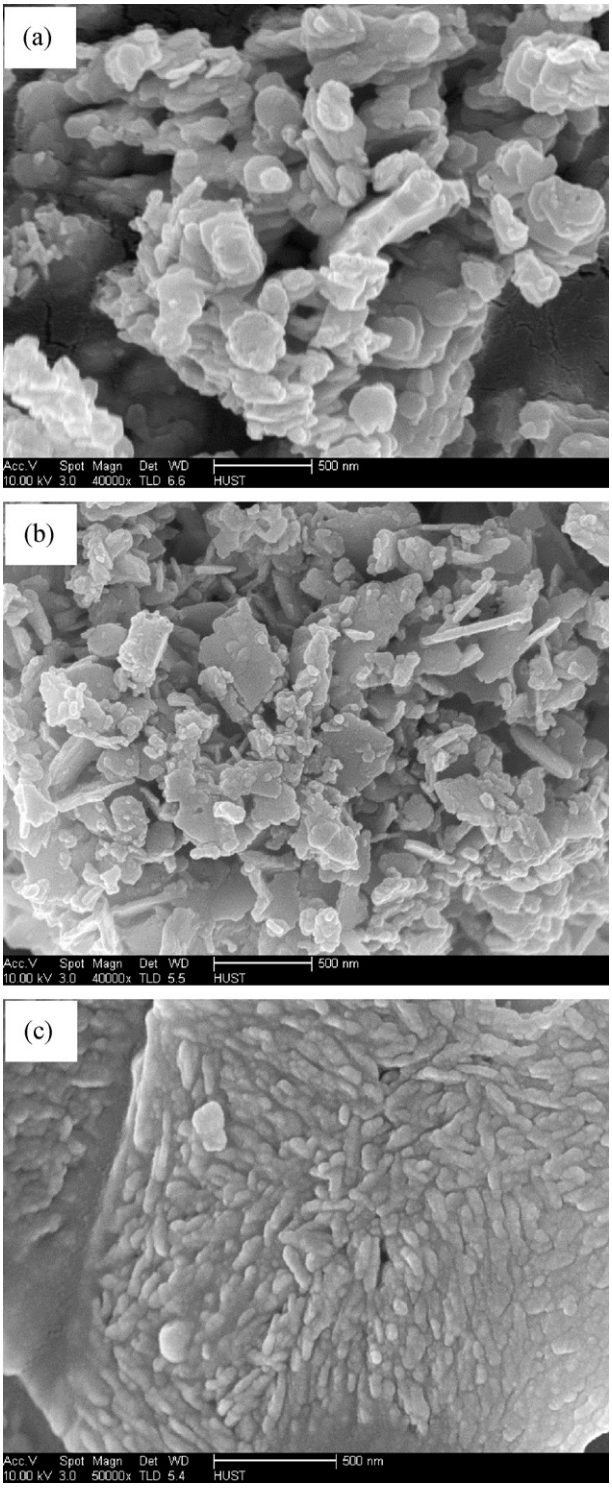

Fig. 13. SEM images of calcination–combustion products at different temperature for 1 h in air: (a) 335 °C, (b) 370 °C, and (c) 430 °C.

results show that the morphology of products converts from sheet to rod-like structure with increasing temperature. The particles are in size range of 100–200 nm at temperature of 370 °C. Agglomeration of the product particulates occurs as calcination temperature is increased.

In order to determine the influence of calcination time, the citrate was calcined at 370 °C for 5 60 min in air. The effect of calcination time on weight loss is shown in Fig. 14. The weight loss remains constant at 47 wt% for a calcination time of 5 min

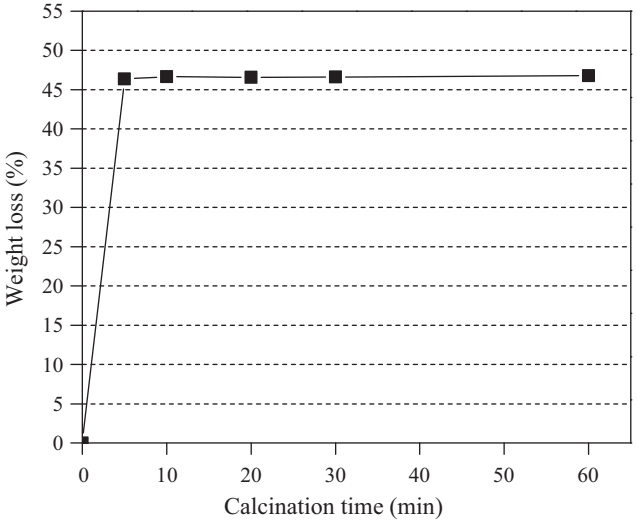

Fig. 14. Effect of the calcination time on weight loss in calcination in air at 370 °C.

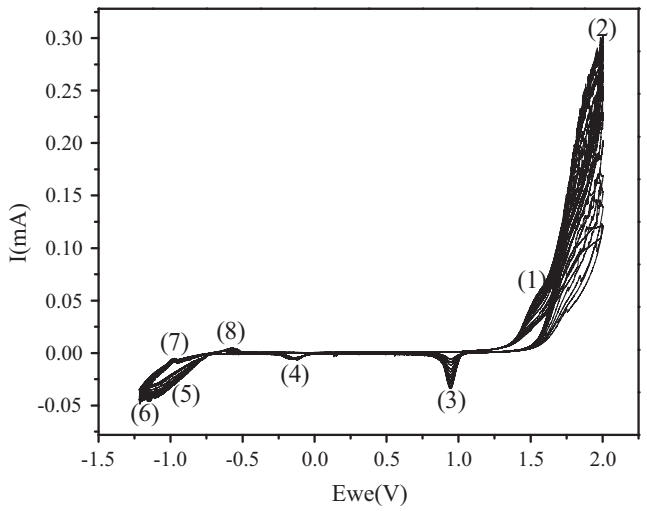

Fig. 16. Cyclic voltammograms of nanostructured lead oxide with 15 cycles of scanning. The sample was synthetized at 370 °C for 20 min in air.

and more. This phenomenon suggests that the reactions during calcination–combustion are fast.

The XRD patterns of combustion product at different calcination time are shown in Fig. 15. A small peak for intermediate can be seen at time of 10 min. However, the peak for the intermediate disappears after 20 min of calcination. Additionally, the XRD patterns show that the diffraction peak for metallic Pb decreases as calcination time is increased, that is, more metallic Pb is oxidized in air. This result suggests that the level of Pb oxidation can be adjusted by control of calcination atmosphere or oxidation potential to achieve a desirable PbO/Pb ratio.

3.5. Characterization of lead oxide with electrochemical technique – cyclic voltammetry

The lead oxide product with nano-size particulate will be used as material for production of lead acid battery. The properties of this kind of products were examined with electrochemical technique – cyclic voltammetry [24]. In the current research, the electrochemical technique was employed to determine the property of nano-size lead oxide produced from the citrate precursor. Fig. 16 shows CV curves for 15 cycles of lead oxide. The lead oxide was synthetized at 370 °C after calcining in air for 20 min and comprised 75 wt% of PbO. In the selected potential range from −1.2 V to 2 V, eight peaks as marked numerically suggest some redox reactions possibly occurring in lead acid battery. The corresponding reactions are shown as described in Eqs. (7)–(14):

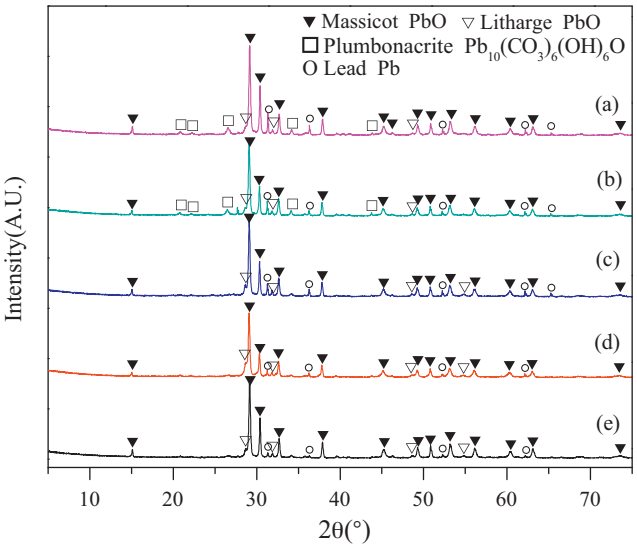

Fig. 15. XRD patterns of calcination–combustion products at 370 °C with different calcination times in air: (a) 5 min, (b) 10 min, (c) 20 min, (d) 30 min, and (e) 60 min.

$$PbSO_4 + 2H_2O \rightarrow PbO_2 + H_2SO_4 + 2H^+ + 2e^- \quad (7)$$

$$2H_2O \rightarrow O_2 + 4H^+ + 2e^- \quad (8)$$

$$PbO_2 + H_2SO_4 + 2H^+ + 2e^- \rightarrow PbSO_4 + 2H_2O \quad (9)$$

$$PbO_2 + 2H^+ + 2e^- \rightarrow PbO + H_2O \quad (10)$$

$$PbSO_4 + 2e^- \rightarrow Pb + SO_4^- \quad (11)$$

$$2H^+ + 2e^- \rightarrow H_2 \quad (12)$$

$$Pb + H_2O \rightarrow PbO + 2H^+ + 2e^- \quad (13)$$

$$Pb + SO_4^- \rightarrow PbSO_4 + 2e^- \quad (14)$$

PbO, WE, converts to $PbSO_4$ in sulfuric acid solution when the scanning goes from −1.2 V towards anodic potentials. It is observed that when the scanning potential in anodic direction reaches $V > 1.2$ V (vs reference electrode), $PbSO_4$ is oxidized to PbO_2 as described in Eq. (7). At the same time under the high potential, evolution of oxygen from the aqueous system takes place, Eq. (8). $PbSO_4$ is also oxidized as well. On the reverse scanning from potential 2.0 V, the reaction (9) occurs at about 1.0 V, that is, PbO_2 is reduced to $PbSO_4$. Some of PbO_2 is then reduced at more cathodic potential around −0.1 V possibly to PbO (Eq. (10)). It can be seen that reduction of $PbSO_4$ to Pb starts at around −0.9 V (Eq. (11)). Under the more negative potential from −0.9 V, hydrogen evolution may take place as described in Eq. (12). On the reverse scanning from the potential of −1.2 V, in anodic direction, a small peak at −0.9 V (Eq. (13)) indicates oxidation of Pb to PbO. The peak around −0.6 V may correspond to oxidation of Pb to $PbSO_4$ (Eq. (14)).

The CV's of nanostructured lead oxide have shown the whole spectrum of possible reactions occurring in lead acid battery. Moreover, the nanostructured lead oxide shows good reversible ability and cycle stability (over 15 cycles), which shows potential applications in lead acid battery.

4. Conclusions

Preparation of nano-structural lead oxide has been investigated by decomposition of lead citrate in inert (nitrogen) and air atmospheres. The lead citrate ($Pb(C_6H_6O_7)\cdot H_2O$), a precursor, was synthesized from spent lead acid battery pastes in citric acid system. The citrate particle was in sheet shape with length of 10–20 μm, width of 2–10 μm and thickness of 0.5 μm. If the calcination was carried out in nitrogen gas, the major decomposition products were orthorhombic phase β-PbO, metallic Pb and elemental C, and the ratio of β-PbO to Pb increased with the increasing temperature. The particle for this product was spherical with a size range 50–60 nm.

When the calcination–combustion was performed in air, lead citrate could be calcined completely at 370 °C within 20 min. Nano size product from calcination–combustion was achieved with particle size of 100–200 nm. It was found to compose mainly of β-PbO with a small part of α-PbO and Pb. The CV's of nanostructured lead oxide shows good reversible ability and cycle stability (over 15 cycles).

Acknowledgments

The authors would like to express thanks to the National Science Council of China (NSC 50804017), Hubei Province Science Fund Distinguished Young Scholars (2011CDA083), and New Century Excellent Talents Project of Ministry of Education (NCET-09-0392) for the financial support. The authors would also like to extend the thanks to Analytical and Testing Center of Huazhong University of Science and Technology (HUST), which supplied the facilities for materials analysis.

References

[1] A. Attar, M. Halali, M. Sobhani, R.T. Ghandehari, Synthesis of titanium nanoparticles via chemical vapor condensation processing, J. Alloys Compd. 509 (2011) 5825–5828.
[2] C.H. Wu, F.S. Chen, S.H. Lin, C.H. Lu, Preparation and characterization of $CuInSe_2$ particles via the hydrothermal route for thin-film solar cells, J. Alloys Compd. 509 (2011) 5783–5788.
[3] D. Devilliers, M.T.D. Thi, E. Mahe, V. Dauriac, N. Lequeux, Electro analytical investigations on electrodeposited lead dioxide, J. Electroanal. Chem. 573 (2004) 227–239.
[4] S. Ghasemi, M.F. Mousavi, H. Karami, M. Shamsipur, S.H. Kazemi, Energy storage capacity investigation of pulsed current formed nano-structured lead dioxide, Electrochim. Acta 52 (2006) 1596–1602.
[5] J. Morales, G. Petkova, M. Cruz, A. Caballero, Synthesis and characterization of lead dioxide active material for lead-acid batteries, J. Power Sources 158 (2006) 831–836.
[6] J. Wang, S. Zhong, G.X. Wang, D.H. Bradhurst, M. Ionescu, H.K. Liu, S.X. Dou, Electrochemical performance of nanocrystalline lead oxide in VRLA batteries, J. Alloys Compd. 327 (2001) 141–145.
[7] M. Cruz, L. Hernan, J. Morales, L. Sanchez, Spray pyrolysis as a method for preparing PbO coatings amenable to use in lead-acid batteries, J. Power Sources 108 (2002) 35–40.
[8] H. Karami, M.A. Karimi, S. Haghdar, A. Sadeghi, R. Mir-Ghaserm, S. Mahdi-Khani, Synthesis of lead oxide nanoparticles by sonochemical method and its application as cathode and anode of lead-acid batteries, Mater. Chem. Phys. 108 (2008) 337–344.
[9] H. Karami, M.A. Karimi, S. Haghdar, Synthesis of uniform nano-structured lead oxide by sonochemical method and its application as cathode and anode of lead-acid batteries, Mater. Res. Bull. 43 (2008) 3054–3065.
[10] M. Salavati-Niasari, F. Mohandes, F. Davar, Preparation of PbO nanocrystals via decomposition of lead oxalate, Polyhedron 28 (2009) 2263–2267.
[11] H. Sadeghzadeh, A. Morsali, V.T. Yilmaz, O. Buyukgungor, Synthesis of PbO nano-particles from a new one-dimensional lead(II) coordination polymer precursor, Mater. Lett. 64 (2010) 810–813.
[12] M.A. Kreusch, M.J.J.S. Ponte, H.A. Ponte, N.M.S. Kaminari, C.E.B. Marino, V. Mymrin, Technological improvements in automotive battery recycling, Resour. Conserv. Recycl. 52 (2007) 368–380.
[13] S. Maruthamuthu, T. Dhanibabu, A. Veluchamy, S. Palanichamy, P. Subramanian, N. Palaniswamy, Elecrokinetic separation of sulphate and lead from sludge of spent lead acid battery, J. Hazard. Mater. 193 (2011) 188–193.
[14] L.C. Ferracin, A.E. Chacon-Sanhueza, R.A. Davoglio, L.O. Rocha, D.J. Caffeu, A.R. Fontanetti, R.C. Rocha-Filho, S.R. Biaggio, N. Bocchi, Lead recovery from a typical Brazilian sludge of exhausted lead-acid batteries using an electrohydrometallurgical process, Hydrometallurgy 65 (2002) 137–144.
[15] M.S. Sonmez, R.V. Kumar, Leaching of waste battery paste components. Part 1: Lead citrate synthesis from PbO and PbO_2, Hydrometallurgy 95 (2009) 53–60.
[16] M.S. Sonmez, R.V. Kumar, Leaching of waste battery paste components. Part 2: leaching and desulphurisation of $PbSO_4$ by citric acid and sodium citrate solution, Hydrometallurgy 95 (2009) 82–86.
[17] R.V. Kumar, V.P. Kotzeva, S. Sonmez, Recovery of lead from lead waste such as lead battery paste, involves treating lead waste with aqueous citric acid solution, separating obtained lead citrate from solution and converting citrate into lead and/or lead oxide, in Cambridge Enterprise Ltd (Uyca) Univ Cambridge Tech Services Ltd (Uyca) WO2008056125-A1.
[18] X.F. Zhu, W.C. Liu, H.Y. Yang, L. Li, J.K. Yang, Preparation of ultrafine PbO powders from lead paste in spent lead acid battery, Chin. J. Nonferrous Met. 20 (2010) 132–136.
[19] G.L. Liu, Introduction to Lead Acid Battery Technology, China Machine Press, Beijing, 2008.
[20] R.R. Hao, X.Y. Fang, S.C. Niu, The Series of Inorganic Chemistry (Third Volume), China Science Press, Beijing, 1988.
[21] M.E. Brown, Thermal decomposition of lead citrate, J. Chem. Soc., Faraday Trans. 69 (1973) 1202–1212.
[22] M.J. Munson, R.E. Riman, Observed phase transformations of oxalate-derived lead monoxide powder, J. Therm. Anal. Calorim. 37 (1991) 2555–2566.
[23] B.P. Jia, L.A. Gao, Synthesis and characterization of single crystalline PbO nanorods via a facile hydrothermal method, Mater. Chem. Phys. 100 (2006) 351–354.
[24] W. Visscher, Cyclic voltammetry on lead electrodes in sulphuric acid solution, J. Power Sources 1 (1977) 257–266.